

Received May 11, 2020, accepted June 9, 2020, date of publication June 19, 2020, date of current version July 1, 2020.

Digital Object Identifier 10.1109/ACCESS.2020.3003702

# WDM-Based Fiber-Optic Time Synchronization Without Requiring Link Calibration

FAXING ZUO<sup>1</sup>, ZUFENG CHEN<sup>1</sup>, LIANG HU<sup>1</sup>, (Member, IEEE),  
JIANPING CHEN<sup>1,2</sup>, (Member, IEEE), AND GUILING WU<sup>1,2</sup>, (Member, IEEE)

<sup>1</sup>State Key Laboratory of Advanced Optical Communication System and Networks, Department of Electronic Engineering, Shanghai Jiao Tong University, Shanghai 200240, China

<sup>2</sup>Shanghai Key Laboratory of Navigation and Location-Based Services, Shanghai 200240, China

Corresponding author: Guiling Wu (wuguilin@sjtu.edu.cn)

This work was supported by the National Natural Science Foundation of China under Grant 61627817.

**ABSTRACT** In this paper, we propose a fiber-optic time synchronization technique based on the bidirectional wavelength division multiplexing (WDM) transmission over a fiber link. The effect of fiber dispersion on the uncertainty of the system is effectively suppressed by properly allocating the forward and backward wavelength maps. Thus, only an initial easy-to-implement calibration in a back-to-back configuration instead of multiple complicated link calibrations is required. To compensate the propagation delay fluctuations, a large-dynamic-range time pre-compensator with high precision is implemented at the local site, enabling a time signal at the remote site is accurately synchronized with the clock at the local site. Our experiments demonstrate that stabilities in terms of time deviation (TDEV) of less than 29.8 ps at 1s and 5.2 ps at 10<sup>4</sup>s and the clock difference of less than 28 ps can be achieved for the fiber link up to 200 km.

**INDEX TERMS** Optical fiber, time synchronization, wavelength division multiplexing, metrology.

## I. INTRODUCTION

High precision fiber-optic time synchronization has attracted extensive research interest over the last two decades in the applications of metrology, telecommunication, navigation and atomic timescales development, where time deviation with the order of pico-second are required, because of fiber-optic's unique advantages of broad bandwidth, low attenuation, and immunity to electromagnetic interference, etc [1]–[3]. The fiber link subjected to the temperature variations and mechanical perturbations, however, leads to the propagation delay of fiber links with the fluctuations, and hence introduces fluctuated delay into the transferred time signal [4]. In order to mitigate this effect, bidirectional time transfer schemes over the single fiber (two-way and round-trip) have been proposed and experimentally demonstrated [5]–[9].

To suppress the effect of Rayleigh backscattering on the bidirectional transferred signal timing jitter, bidirectional wavelength-division multiplexing (WDM) schemes have been widely adopted [10]–[16]. However, unlike frequency dissemination, not only stability but accuracy is also a very vital index for time synchronization. Therefore, the existing WDM based schemes require a high precision link

calibration procedure to determine the bidirectional delay asymmetry of the fiber link arose from the chromatic dispersion and its temperature-dependent delay variations for different wavelengths in the forward and backward directions. The fiber link calibration can be performed by employing the empirical value of the chromatic dispersion coefficient or refractive indexes of the corresponding fiber [10], [11]. In practical applications, however, the urban fiber links are often connected by several different sections, which are typically supplied by different companies, resulting in the inaccurate empirical value for the field-deployed fiber links. Another method of the link calibration, based on the measurement of the chromatic dispersion of the whole fiber link in filed by shifting laser wavelengths, may enhance the synchronization accuracy [17]. However, the calibration method is complicated, and recalibration is necessary for any change of fiber links, which will increase the operation and maintenance cost.

In this paper, we propose a fiber-optic time synchronization scheme based on the bidirectional wavelength division multiplexing (WDM) transmission without requiring any complex optical-fiber link calibrations. The effect of the fiber dispersion on the uncertainty of the system is effectively suppressed by properly allocating the bidirectional wavelengths. Time synchronization between the local and remote sites is realized by a large-dynamic-range time pre-compensator.

The associate editor coordinating the review of this manuscript and approving it for publication was Rene Essiambre.

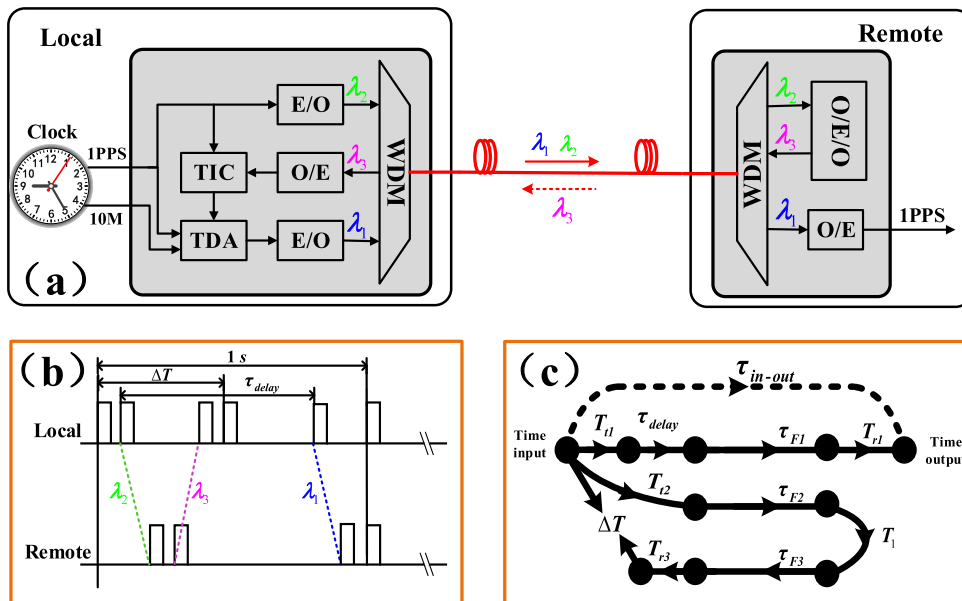


**FIGURE 1.** (a) Diagram of the proposed time synchronization scheme over a point-to-point fiber link based on the wavelength-division multiplexing technique, (b) The operation sequence flow, (c) The timing model of the scheme. TIC: time interval counter, TDA: time delay adjuster, WDM: wavelength division multiplexer, E/O: electrical-optical converter, O/E: optical-electrical converter, O/E/O: optical-electrical-optical converter.

The experimental results show that uncertainty of less than 28 ps can be reached with the proposed scheme for the fiber link up to 200 km which is consistent with the theoretical analysis, and stabilities in terms of time deviation (TDEV) can be less than 29.8 ps at 1 second and 5.2 ps at  $10^4$  seconds.

## II. PRINCIPLE

Figure 1(a) illustrates the diagram of the proposed time synchronization scheme. The operation sequence flow is shown in Fig. 1(b). The time signal (1PPS, one-pulse-per-second) at the local site is sent to the remote site over an optical carrier with a wavelength of  $\lambda_2$  via an optical fiber. At the remote site, the received time signal is then returned to the local site on a wavelength of  $\lambda_3$  over the same fiber after processing with the optical-electrical-optical (O/E/O) conversion. The time difference between the local 1PPS and the received one at the local site is measured by a time interval counter (TIC), which is then used to control the time delay adjuster (TDA) to pre-compensate the propagation delay fluctuations introduced by the optical fiber. The pre-compensated time signal is sent to the remote site over another optical carrier with a wavelength of  $\lambda_1$  to obtain a time synchronized signal at the remote site.

The timing model indicating the time delay of each part is shown in Fig. 1(c).  $T_{t1}$  ( $T_{t2}$ ) and  $T_{r1}$  ( $T_{r3}$ ) are the sending and receiving delays of the time signal at the local (remote) site,  $T_1$  denotes the O/E/O conversion delay at the remote site; Considering the propagation delays of electronic circuits, internal cables, optical to electrical conversion and electrical to optical conversion, we can take the fluctuations of the delays (i.e.  $T_{t1}$ ,  $T_{t2}$ ,  $T_{r1}$ ,  $T_{r3}$ ,  $T_1$ ) as constants.  $\tau_{F1}$ ,  $\tau_{F2}$ ,  $\tau_{F3}$  are the forward or backward propagation delays in the fiber link for different wavelengths,  $\tau_{delay}$  is the pre-compensation

delay of the time signal achieved by TDA,  $\Delta T$  represents the measured time difference by TIC,  $\tau_{in-out}$ , indicated by the dashed arrow, is the time difference between the local clock and the output at the remote site, which should be one second when the remote site is exactly synchronized with the local site.

The system is initially calibrated by connecting the local site and the remote site with a short optical fiber (2m). In this situation, time synchronization between the local site and the remote site is achieved by adjusting the pre-compensation delay in TDA to make  $\tau_{in-out}$  to be one second. Thus, we have,

$$\Delta T^0 = T_{t2} + \tau_{F2}^0 + T_1 + \tau_{F3}^0 + T_{r3}, \quad (1)$$

$$\tau_{in-out}^0 = 1 = T_{t1} + \tau_{delay}^0 + \tau_{F1}^0 + T_{r1}, \quad (2)$$

where  $\tau_{delay}^0$  and  $\Delta T^0$  represent the pre-compensation delay and the measured time interval achieved by TIC,  $\tau_{F1}^0$ ,  $\tau_{F2}^0$  and  $\tau_{F3}^0$  represent the propagation delays of the short fiber link in this back-to-back configuration for different wavelengths, respectively.

Similarly, when the local site and the remote site are connected by a fiber link with a length of  $L$ , we can have,

$$\Delta T^L = T_{t2} + \tau_{F2}^L + T_1 + \tau_{F3}^L + T_{r3}, \quad (3)$$

$$\tau_{in-out}^L = T_{t1} + \tau_{delay}^L + \tau_{F1}^L + T_{r1}, \quad (4)$$

where  $\tau_{delay}^L$  and  $\Delta T^L$  represent the pre-compensation delay and the measured time difference countered by TIC,  $\tau_{F1}^L$ ,  $\tau_{F2}^L$  and  $\tau_{F3}^L$  represent the propagation delays of the fiber link  $L$  for different wavelengths, respectively.

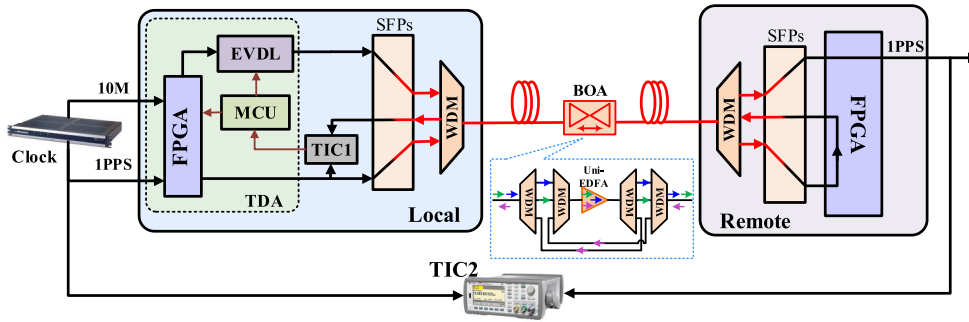


**FIGURE 2.** Experiment setup for the proposed time synchronization scheme. The inset shows the structure of the bidirectional optical amplifier (the transmission time for wavelength paths in blue, green and pink of the BOA are equal). TDA: time delay adjuster, FPGA: field programmable gate array, MCU: micro control unit, SFP: small form-factor pluggable transceiver, EVDL: electronic variable delay line, TIC: time interval counter, WDM: wavelength division multiplexer, BOA: bidirectional optical amplifier, Uni-EDFA: unidirectional erbium doped fiber amplifier.

From Eq. 1-4, we can obtain,

$$\tau_{in-out}^L = \tau_{in-out}^0 + \frac{\Delta T^L - \Delta T^0}{2} + \left( \tau_{delay}^L - \tau_{delay}^0 \right) + \left( \tau_{F1}^L - \frac{\tau_{F2}^L + \tau_{F3}^L}{2} \right) + \left( \frac{\tau_{F2}^0 + \tau_{F3}^0}{2} - \tau_{F1}^0 \right), \quad (5)$$

Considering that  $\tau_{F1}^0$ ,  $\tau_{F2}^0$  and  $\tau_{F3}^0$  are equal virtually in the back-to-back configuration, the fifth term on the right-side of Eq. 5 can be ignored. The fourth term mainly comes from the wavelength difference between the forward and backward directions in the fiber link  $L$ . When the gaps among the three wavelengths are narrow enough, for example, 0.4 nm or 0.8 nm for the WDM optical transmission standards [18], the chromatic dispersion coefficients for the three wavelengths are considered to be equal and can be expressed by  $D$ . Thus we have,

$$\left( \tau_{F1}^L - \frac{\tau_{F2}^L + \tau_{F3}^L}{2} \right) = LD \left( \lambda_1 - \frac{\lambda_2 + \lambda_3}{2} \right). \quad (6)$$

From Eq. 6, we can see that the fourth term in Eq. 5 can also be neglected when  $\lambda_1 - (\lambda_2 + \lambda_3)/2 = 0$ , and Eq. 5 can be simplified into

$$\tau_{in-out}^L = 1 + \frac{\Delta T^L - \Delta T^0}{2} + \left( \tau_{delay}^L - \tau_{delay}^0 \right). \quad (7)$$

As illustrated in Eq. 7, time synchronization between the local site and the remote site can be achieved by adjusting  $\tau_{delay}^L$  to make  $\tau_{in-out}^L = 1$  s according to the known values of  $\Delta T^0$ ,  $\tau_{delay}^0$  and  $\Delta T^L$ . One can also see that the time synchronization in the case is independent of the length and the chromatic dispersion coefficient of the optical fiber link. In other words, the proposed scheme, in addition to suppressing backscattering, can achieve time synchronization without requiring link calibration by selecting pre-defined wavelengths.

### III. EXPERIMENT APPARATUS AND RESULTS

The experiment setup for the proposed scheme is illustrated in Fig. 2. At the local site, the 1PPS time signal from a Rb

clock is encoded into a time code in a field programmable gate array (FPGA) as proposed in [19], and injected into the fiber link through a WDM module with the assistance of a small form-factor pluggable transceiver (SFP) with a wavelength of  $\lambda_2 = 1548.52$  nm. At the remote site, a SFP is used to detect the time signal over the wavelength of  $\lambda_2$ , and send it back over the same fiber link with a wavelength of  $\lambda_3 = 1550.12$  nm by a direct optical-electrical-optical conversion. The time interval between the local input 1PPS and the returned back one at the local site is determined by TIC1. A micro control unit (MCU) is used to control the time pre-compensation delay adjustment according to the values of  $\Delta T^0$ ,  $\tau_{delay}^0$  and  $\Delta T^L$ . The pre-compensator consists of a large range adjustable delay and a small range adjustable delay with a high resolution implemented in FPGA and EVDL (electronic variable delay line), respectively, similar with the one adopted in [11]. The large time delays with a resolution of 8 ns are implemented in the FPGA with a working clock of 125 MHz synchronized to the 10 MHz frequency reference of the Rb clock. The EVDL has a tuning rang of 10.6 ns in a 10 ps resolution. The pre-compensated 1PPS time signal is transferred to the remote site over a wavelength of  $\lambda_1 = 1549.32$  nm. Note that the three wavelengths employed here satisfy conditions to neglect the fourth term in Eq.5, and Eq.7 can be used. To evaluate the synchronization performance, another TIC2 is used to measure the time interval between the 1PPS of the local clock and the synchronized time signal output at the remote site.

Figure 3 shows the measured clock difference between the local and remote sites in a 50 km fiber link over 80000 seconds with and without synchronization, respectively. For the case without synchronization (i.e. one way transfer), the measured clock difference varies within a range of about 6 ns around an average of about 239381.307 ns. On the contrast, the measured clock difference over the fiber link with synchronization varies around 12 ps with a peak-to-peak value of less than 252 ps, indicating that time synchronization between the local and remote sites has been successfully achieved. Time synchronization can extend to 100 km without requiring optical amplification

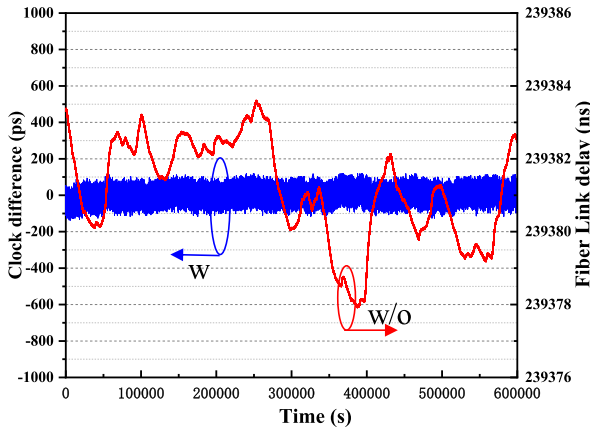


**FIGURE 3.** Measured clock differences over 50 km fiber link with/without time synchronization.

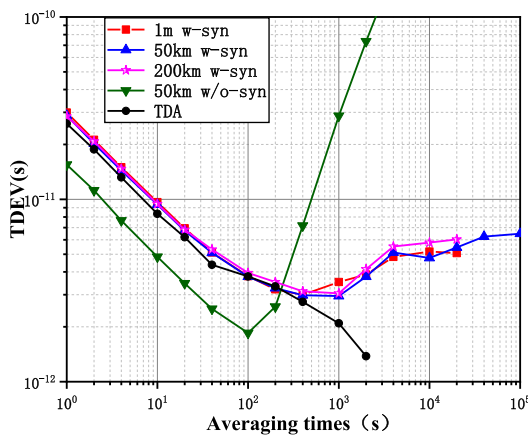


**FIGURE 4.** Measured stability in terms of TDEV with and without time synchronization for different fiber link lengths. As a comparison, the stability of TDA for time delay pre-compensation is also shown.

in the fiber link. We also verified the performance of the system in 200 km optical fiber link by employing a wavelength-division bidirectional optical amplifier (BOA) as proposed in [20], shown in the inset of Fig. 2. In order to guarantee the bidirectional symmetry of the BOA, the time delay differences among the three optical fiber paths are precisely adjusted by the optical tunable delay lines with a precision of 0.01 ps.

The measured stabilities in terms of TDEV over 1 m, 50 km and 200 km fiber links with time synchronization are shown in Fig. 4. As a comparison, the stability of the propagation delay of 50 km fiber link without synchronization is also presented. The result of 1 m can be regarded as the noise floor of our experimental apparatus. One can see that the stabilities of both 50 km and 200 km synchronized links are less than 29.8 ps at one second and 5.4 ps at  $10^4$  seconds and close to the noise floor. The long-term stabilities are significantly improved compared to the 50 km non-synchronized link, which indicate that the time delay fluctuations of the optical fiber is well compensated. It is important to note that the short-term (1-100 s) stability of the synchronized links, even in the back-to-back configuration, is mainly limited by that

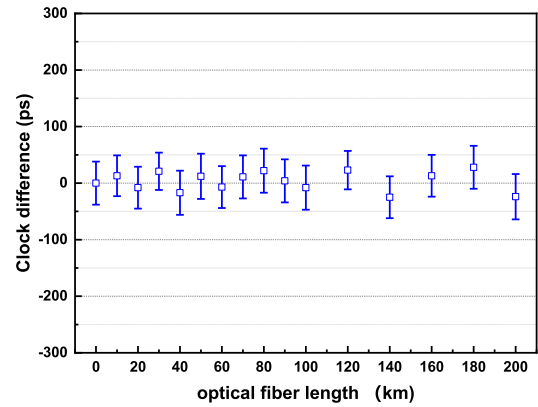


**FIGURE 5.** Measured clock difference for different fiber link lengths.

of the added TDA for pre-compensation (see the dotted curve in Fig.4), and is worse than that of the non-synchronized link. TDA with higher stabilities is required for improving the short-term (1-100 s) stability of the synchronized links.

The clock differences over various fiber lengths are shown in Fig. 5. In these measurements, after the initial calibration with a short fiber, no link calibration operation is performed for the different fiber link lengths. We can see that the the maximum mean clock difference is less than 28 ps for the fiber links up to 200 km, demonstrating that the proposed scheme is able to realize high-accuracy time synchronization without requiring link calibrations.

#### IV. UNCERTAINTY ANALYSIS

The main terms of the uncertainty budget for the proposed time synchronization scheme are summarized in Tab. 1. Here, type A uncertainty is evaluated by the statistical analysis of series of experiment observations, while type B uncertainty is data collected from non-experiment, such as data sheets, calibration reports and journal articles, etc [21], [22].

The first term results from the initial calibration in the back-to-back time synchronization configuration. A standard deviation of the clock difference of 30.55 ps is determined for 200 independent measurements, which indicates a type A uncertainty of 2.16 ps [21]. The second term is coming from TIC for determining the round-trip propagation delay. The type B uncertainty of TIC used in the experiment is 20 ps.

The third and forth terms denote the uncertainty originating from the time pre-compensation delay adjustment, which consists of the delay implemented in FPGA and in EVDL. To effectively evaluate this uncertainty coming from FPGA, we control FPGA to achieve the time delay from 0 to 1 s in a 0.1 s step and examine the differences between the measured time interval and the expected one. The evaluation result is shown in Fig. 6(a), and a type A uncertainty of 5.12 ps is obtained. Similarly, the uncertainty coming from EVDL is evaluated by adjusting the delay from 0 to 8 ns in a 1 ns step (shown in Fig. 6 (b)), and a type A uncertainty of 10.12 ps is acquired. Meanwhile, the resolution of 10 ps is another type B uncertainty source for EVDL. Consequently, a combined uncertainty is 14.23 ps for the delay in EVDL.

TABLE 1. Uncertainty budget for the proposed time synchronization scheme.

Uncertainty source	Coefficient	Estimated value	Uncertainty contribution (ps)	Uncertainty type
Calibration	1	2.16 ps	2.16	A
TIC	1	20 ps	20	B
Counting delay	1	5.12 ps	5.12	A
Delay by EVDL	1	14.23 ps	14.23	A&B
Wavelength difference	$DL^*$	4.3 pm	$4.3 \times 10^{-3}DL$	A
Dispersion coefficient	$0.8^2L$	0.1 ps/nm <sup>2</sup> /km	$0.064L$	B
PMD	$\sqrt{3}\sqrt{L}$	0.05ps/ $\sqrt{\text{km}}$	$0.05\sqrt{3}\sqrt{L}$	B
Sagnac effect	1	1.2	1.2	B

\* The units of  $D$  and  $L$  are ps/nm/km and km, respectively.

TABLE 2. The theoretical uncertainty and the measured clock difference.

Fiber length (km)	10	50	100	180	200
Theoretical uncertainty (ps)	$\pm 25.2$	$\pm 25.7$	$\pm 27.1$	$\pm 30.7$	$\pm 31.8$
Measured clock difference (ps)	13	12	-8	28	-24

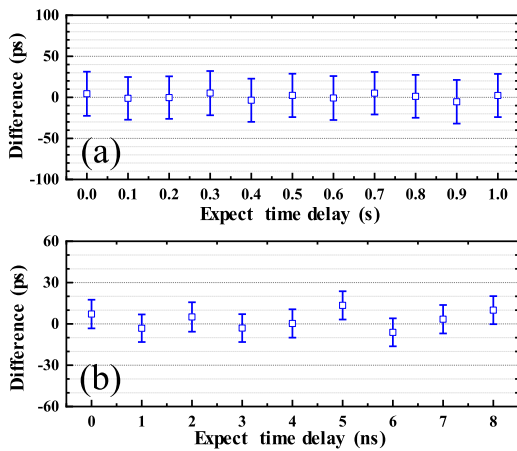


FIGURE 6. Time difference between the measured delay and the expected value implemented in FPGA (a) and in EVDL (b).

This part uncertainty can be reduced by employing higher precision EVDLs.

The wavelength-difference dependent fiber chromatic dispersion is another source of the uncertainty [23]. In practice, the wavelengths of SFPs cannot be completely accurate and stable for the limitation of the practical manufacture technique and the temperature variations. Figure 7 shows the wavelengths of the three employed SFP transceivers measured by an optical wavelength meter with a resolution of 0.1 pm. It can be seen that the wavelengths vary within a range of 3.5 pm in 100000 seconds. Since the wavelength variations of the three SFPs are independent, the overall contribution is  $4.3 \text{ pm} (\sqrt{3.5^2 + (3.5/2)^2} \times 2)$ , according to Eq.6, resulting in an uncertainty of  $4.3 \times 10^{-3}DL$  ps for the fiber length of  $L$  km. Moreover, another uncertainty source comes from the approximation that the chromatic dispersion coefficients of the three wavelengths,  $D$ , are equal. An uncertainty of  $0.064L$  ps will be introduced for a dispersion slope of 0.1 ps/nm<sup>2</sup>/km which exceeds the values of most commercial fibers and represents the worse case [24].

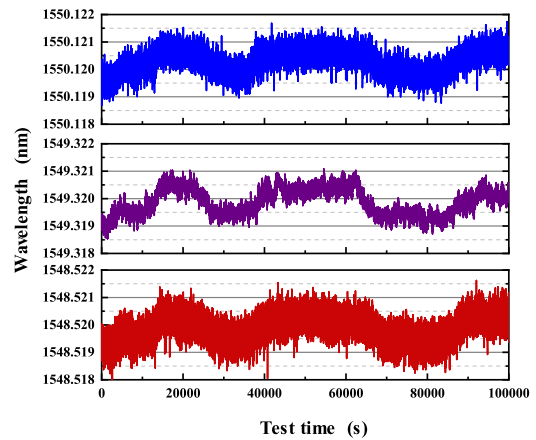


FIGURE 7. Measured wavelengths of the three SFP transceivers.

The uncertainty from the random polarization mode dispersion (PMD) is calculated with the coefficient of 0.05ps/ $\sqrt{\text{km}}$  [22]. The last term represents the uncertainty introduced by the Sagnac effect concerning the impact of the Earth’s rotation. The uncertainty from the correction of the Sagnac effect is less than 1.2 ps for any two sites connected with the fiber link of 200 km when the position uncertainty is better than 1 km of any point located on the earth, which can be achieved thanks to the global positioning system (GPS) [25].

The uncertainty caused by the bidirectional optical amplifier (BOA) is negligible since the time delay differences among the three wavelength paths are precisely controlled with a precision of 0.01 ps.

According to above analysis, the calculated combined uncertainty for the proposed time synchronization scheme over different fiber lengths without any fiber link calibration is summarized in Table 2. One can see that the uncertainty increases slightly with the extension of fiber links and still no more than 31.8 ps for the fiber links up to 200 km. The measured clock differences over different fiber links



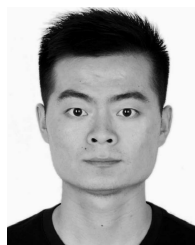
after synchronization are also listed. It can be seen that all the measured clock differences are within the calculated uncertainty.

## V. CONCLUSION

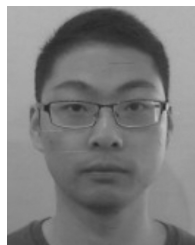
In summary, we propose and implement a fiber-optic time synchronization scheme without the need of fiber link calibrations and only a calibration in the back-to-back configuration is required. With the proposed scheme, a time signal (PPS) can be obtained at the remote site, which is synchronized with the one of the local site. Different factors related to the uncertainty of the time synchronization system are investigated in detail and full uncertainty budgets for the system are calculated. The results illustrate that the mean clock difference of less than 28 ps and the stabilities in terms of TDEV of less than 29.8 ps at one second and 5.2 ps at  $10^4$  seconds can be achieved for the fiber links up to 200 km.

## REFERENCES

- [1] J. Grotti *et al.*, "Geodesy and metrology with a transportable optical clock," *Nature Phys.*, vol. 14, no. 5, pp. 437–441, May 2018.
- [2] C. Lisdat *et al.*, "A clock network for geodesy and fundamental science," *Nature Commun.*, vol. 7, p. 12443, Aug. 2016.
- [3] L. Hu, N. Poli, L. Salvi, and G. M. Tino, "Atom interferometry with the Sr optical clock transition," *Phys. Rev. Lett.*, vol. 119, no. 26, Dec. 2017, Art. no. 263601.
- [4] Ł. Śliwczyński, P. Krehlik, and M. Lipiński, "Optical fibers in time and frequency transfer," *Meas. Sci. Technol.*, vol. 21, no. 7, Jul. 2010, Art. no. 075302.
- [5] S. R. Jefferts, M. A. Weiss, J. Levine, S. Dilla, E. W. Bell, and T. E. Parker, "Two-way time and frequency transfer using optical fibers," *IEEE Trans. Instrum. Meas.*, vol. 46, no. 2, pp. 209–211, Apr. 1997.
- [6] H. Liang, G. Wu, Z. Hao, and J. Chen, "A 300-kilometer optical fiber time transfer using bidirectional TDM dissemination," in *Proc. 46th Annu. Precise Time Time Interval Syst. Appl. Meeting*, Dec. 2014, pp. 41–44.
- [7] K. Liang, A. Zhang, Z. Yang, W. Chen, W. Wang, L. Bai, and G. Fu, "Preliminary time transfer through optical fiber at NIM," in *Proc. Joint Conf. IEEE Int. Freq. Control Symp. Eur. Freq. Time Forum*, Apr. 2015, pp. 742–746.
- [8] B. Wang, C. Gao, W. L. Chen, J. Miao, X. Zhu, Y. Bai, J. W. Zhang, Y. Y. Feng, T. C. Li, and L. J. Wang, "Precise and continuous time and frequency synchronisation at the  $5 \times 10^{-19}$  accuracy level," *Sci. Rep.*, vol. 2, no. 1, p. 556, Dec. 2012.
- [9] V. Smotlacha, A. Kuna, and W. Mache, "Time transfer in optical network," in *Proc. 42nd Annu. Precise Time Time Interval (PTTI) Meeting*, 2010, pp. 427–436.
- [10] N. Kaur, P. Tuckey, and P. E. Pottie, "Time transfer over a white rabbit network," in *Proc. Eur. Freq. Time Forum (EFTF)*, Apr. 2016, pp. 1–4.
- [11] L. Yu, R. Wang, L. Lu, Y. Zhu, C. Wu, B. Zhang, and Y. Wei, "Large-dynamic-range time pre-compensation scheme for fiber optic time transfer," *Appl. Opt.*, vol. 56, no. 6, p. 1757, 2017.
- [12] W. Chen, Q. Liu, N. Cheng, D. Xu, F. Yang, Y. Gui, and H. Cai, "Joint time and frequency dissemination network over delay-stabilized fiber optic links," *IEEE Photon. J.*, vol. 7, no. 3, pp. 1–9, Jun. 2015.
- [13] O. Lopez, C. Chardonnet, A. Amy-Klein, A. Kanj, P.-E. Pottie, D. Rovera, J. Achkar, and A. G. Santarelli, "Simultaneous remote transfer of accurate timing and optical frequency over a public fiber network," in *Proc. Joint Eur. Freq. Time Forum Int. Freq. Control Symp. (EFTF/IFC)*, Jul. 2013, vol. 110, no. 1, pp. 3–6.
- [14] M. Rost, D. Piester, W. Yang, T. Feldmann, T. Wübbena, and A. Bauch, "Time transfer through optical fibres over a distance of 73 km with an uncertainty below 100 ps," *Metrologia*, vol. 49, no. 6, pp. 772–778, Oct. 2012.
- [15] J. Vojtech, O. Havlis, M. Slapak, P. Skoda, V. Smotlacha, R. Velc, P. Munster, J. Kundrat, M. Altmann, J. Radil, L. Altmannova, R. Vohnout, M. Hazlinsky, T. Horvath, R. Slavik, M. Cizek, L. Pravidova, S. Rerucha, J. Hrabina, and O. Cip, "Joint stable optical frequency and precise time transfer over 406 km of shared fiber lines—Study," in *Proc. 40th Int. Conf. Telecommun. Signal Process. (TSP)*, Jul. 2017, pp. 694–697.
- [16] S.-C. Ebenhag, P. O. Hedekvist, P. Jarlemark, R. Emardson, K. Jaldehag, C. Rieck, and P. Löthberg, "Measurements and error sources in time transfer using asynchronous fiber network," *IEEE Trans. Instrum. Meas.*, vol. 59, no. 7, pp. 1918–1924, Jul. 2010.
- [17] P. Krehlik, L. Śliwczynski, L. Buczek, and J. Kolodziej, "Fiber-optic UTC(k) timescale distribution with automated link delay cancellation," *IEEE Trans. Ultrason., Ferroelectr., Freq. Control*, vol. 66, no. 1, pp. 163–169, Jan. 2019.
- [18] *Spectral Grids for WDM Applications: DWDM Frequency Grid*, document ITU-T G.694.1, 2003.
- [19] G. Wu, L. Hu, H. Zhang, and J. Chen, "High-precision two-way optical-fiber time transfer using an improved time code," *Rev. Sci. Instrum.*, vol. 85, no. 11, Nov. 2014, Art. no. 114701.
- [20] X. Ding, G.-L. Wu, F.-X. Zuo, and J.-P. Chen, "Bidirectional optical amplifier for time transfer using bidirectional WDM transmission," *Optoelectron. Lett.*, vol. 15, no. 6, pp. 401–405, Nov. 2019.
- [21] *Evaluation of Measurement Data-Guide to the Expression of Uncertainty in Measurement*, BIPM, IEC, IFCC, ILAC, ISO, IUPAC, IUPAP, OIML, JCGM, Jan. 2008.
- [22] H. Zhang, G. Wu, X. Li, and J. Chen, "Uncertainty analysis of BTDM-SFSW based fiber-optic time transfer," *Metrologia*, vol. 54, no. 1, pp. 94–101, Feb. 2017.
- [23] E. Samain, P. Exertier, C. Courde, P. Fridelance, P. Guillemot, M. Laas-Bourez, and J.-M. Torre, "Time transfer by laser link: A complete analysis of the uncertainty budget," *Metrologia*, vol. 52, no. 2, pp. 423–432, Apr. 2015.
- [24] P. S. André and A. N. Pinto, "Chromatic dispersion fluctuations in optical fibers due to temperature and its effects in high-speed optical communication systems," *Opt. Commun.*, vol. 246, nos. 4–6, pp. 303–311, Feb. 2005.
- [25] H. Zhang, G. Wu, L. Hu, X. Li, and J. Chen, "High-precision time transfer over 2000-km fiber link," *IEEE Photon. J.*, vol. 7, no. 6, pp. 1–9, Dec. 2015.



**FAXING ZUO** was born in Liaocheng, Shandong, China, in 1994. He received the B.S. degree in communication engineering from Xidian University, Xi'an, China, in 2017. He is currently pursuing the Ph.D. degree with the State Key Laboratory of Advanced Optical Communication Systems and Networks, Department of Electronic Engineering, Shanghai Jiao Tong University, China. His current research interests include fiber-optic time and frequency transmission.



**ZUFENG CHEN** received the B.S. degree from the Wuhan University of Technology, China, in 2016. He is currently pursuing the degree with the State Key Laboratory of Advanced Optical Communication Systems and Networks, Department of Electronic Engineering, Shanghai Jiao Tong University, China. His current research interest includes fiber-optic time transmission.



**LIANG HU** (Member, IEEE) received the B.S. degree from Hangzhou Dianzi University, China, in 2011, the M.S. degree from Shanghai Jiao Tong University, China, in 2014, and the Ph.D. degree from the University of Florence, Italy, in 2017. He was a Marie-Curie Early Stage Researcher with FACT project. He is currently a Tenure-Track Assistant Researcher with the State Key Laboratory of Advanced Optical Communication Systems and Networks, Department of Electronic Engineering, Shanghai Jiao Tong University. His current research interests include photonic signal transmission and atom interferometry.



**JIANPING CHEN** (Member, IEEE) received the B.S. degree from Zhejiang University, China, in 1983, and the M.S. and Ph.D. degrees from Shanghai Jiao Tong University, China, in 1986 and 1992, respectively. He is currently a Professor with the State Key Laboratory of Advanced Optical Communication Systems and Networks, Department of Electronic Engineering, Shanghai Jiao Tong University. He is also a Principal Scientist of the National Basic Research Program of China (also known as 973 Program). His main research interests include opto-electronic devices and integration, photonic signal processing, and system applications.



**GUILONG WU** (Member, IEEE) received the B.S. degree from the Haer Bing Institute of Technology, China, in 1995, and the M.S. and Ph.D. degrees from the Huazhong University of Science and Technology, China, in 1998 and 2001, respectively. He is currently a Professor with the State Key Laboratory of Advanced Optical Communication Systems and Networks, Department of Electronic Engineering, Shanghai Jiao Tong University, China. His current research interest includes photonic signal processing and transmission.

• • •